

**Adaptive evolution on a continuous lattice model**

Elder S. Claudino, M. L. Lyra, and Iram Gleria

*Instituto de Física, Universidade Federal de Alagoas, 57072-970 Maceió-AL, Brazil*

Paulo R. A. Campos\*

*Departamento de Física, Universidade Federal de Pernambuco, 52171-900 Recife-PE, Brazil*

(Received 29 November 2012; revised manuscript received 25 January 2013; published 15 March 2013)

In the current work, we investigate the evolutionary dynamics of a spatially structured population model defined on a continuous lattice. In the model, individuals disperse at a constant rate  $v$  and competition is local and delimited by the competition radius  $R$ . Due to dispersal, the neighborhood size (number of individuals competing for reproduction) fluctuates over time. Here we address how these new variables affect the adaptive process. While the fixation probabilities of beneficial mutations are roughly the same as in a panmictic population for small fitness effects  $s$ , a dependence on  $v$  and  $R$  becomes more evident for large  $s$ . These quantities also strongly influence fixation times, but their dependencies on  $s$  are well approximated by  $s^{-1/2}$ , which means that the speed of the genetic wave front is proportional to  $\sqrt{s}$ . Most important is the observation that the model exhibits a dual behavior displaying a power-law growth for the fixation rate and speed of adaptation with the beneficial mutation rate, as observed in other spatially structured population models, while simultaneously showing a nonsaturating behavior for the speed of adaptation with the population size  $N$ , as in homogeneous populations.

DOI: [10.1103/PhysRevE.87.032711](https://doi.org/10.1103/PhysRevE.87.032711)

PACS number(s): 87.23.Kg, 87.10.Mn, 02.50.Ey

**I. INTRODUCTION**

A long-standing question in theoretical population biology regards the role that deterministic evolutionary forces and stochasticity play in adapting populations [1,2]. In recent decades, we have seen a significant rise in studies of experimental evolution, which provide long-term data sets under controlled conditions [3,4]. These studies allowed for a correct inference of the range of mutation rates and distribution of fitness effects in real microorganism populations [5,6]. The results had significant consequences for the current understanding of the adaptive process in natural populations and highlighted the need for new theoretical approaches to address this issue [8,33].

It is well established that an increase in adaptation results from the spread of beneficial alleles through the whole population, after these mutations have been able to overcome genetic drift. In asexual populations, this process is complicated by interference among selected mutations. This so-called clonal interference slows down the rate of adaptation since co-occurring mutations arising in different individuals have to compete for fixation and all but one of them are ultimately lost [7]. A second effect appears when the beneficial mutations arise very frequently. Under these circumstances, multiple mutations accumulate in the same lineage before the first mutation fixes, and thus a multiple-mutant (a mutant that carries two or more segregating beneficial mutations) benefits from their combined effects [8]. In sexual populations, interference still affects the fate of beneficial mutations, but its effect on the rate of adaptation is weaker [17,18], because mutations in different lineages can recombine into the same individual (the Fisher-Muller hypothesis for the advantage of sex [2,9]).

In recent years, statistical physics modeling has been used to uncover several emerging characteristics of evolving populations such as symmetry breaking, pattern formation, and self-organization [10–16]. In addition, there has been a growing interest in investigating adaptation in spatially structured populations [19,20,22,23,39], such as microbial biofilms [24,25]. Their dynamics depart from those of well-mixed populations and they also seem to provide an appropriate model of cancer progression [23]. Empirical observations show that imposing spatial structure alters the rate of fixation of advantageous mutations [21,26], even though theoretical models predict that the probability of establishment (i.e., of overcoming genetic drift) is independent of spatial structure at least under certain conditions [27,28]. The reason is that, in structured populations beneficial mutations spread at a much slower pace [20,21,29], which enhances the chance of competition among established mutations and, hence, increases clonal interference.

In the current work, we propose a model for adaptive evolution of a spatially structured population, but rather than supposing an integer discrete lattice as in previous works [20,21], here we assume a continuous lattice model. In this approach the size of the neighborhood, which defines the spatial range over which species interact through natural selection, is a parameter. Dispersal of individuals over the lattice occurs at a constant rate, such that the neighborhood composition can change continuously. The proposed model advances the current framework of the emerging field of landscape genetics [30–32], since dispersal in the homogeneous environment, like the one assumed here, can provide a useful guide for comparison with works that aims to investigate the speed of adaptation in landscapes with a complex structure.

**II. THE MODEL**

In what follows, the population will be considered to consist of  $N$  individuals randomly distributed over a continuous square

\*prac@df.ufpe.br

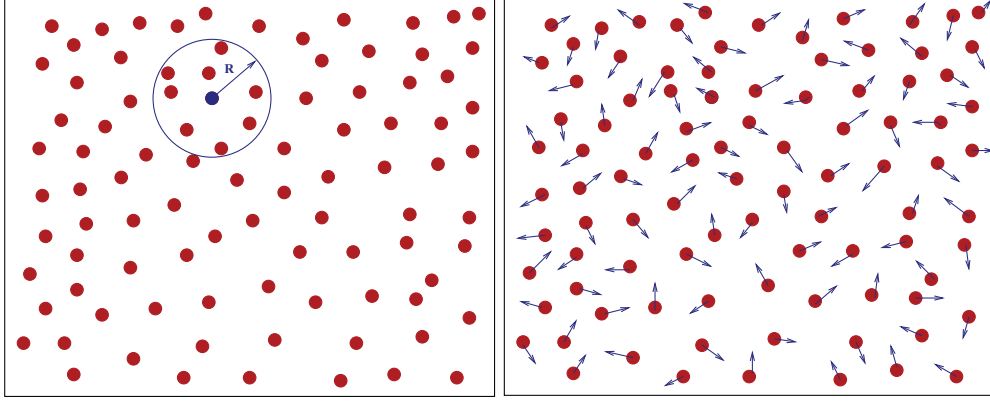


FIG. 1. (Color online) Illustration of the model. Left panel:  $N$  individuals are distributed on a continuous lattice of size  $L$ . Henceforth, we set  $L = 1$ , such that  $N$  corresponds to the density of individuals per unit area. The model assumes nonoverlapping generations. In each generation, individuals die and are replaced by offspring from neighboring individuals: All individuals within the area delimited by the competition radius  $R$  (centered around the individual to be replaced) are candidates to produce the offspring that will occupy the position of the focal individual to be replaced. The probability of producing offspring is proportional to each individual's fitness. During reproduction, beneficial mutations occur at a constant rate  $U_b$ . Right panel: After the reproduction stage, individuals diffuse over the lattice by a constant distance  $v$  but in a random direction  $\theta \in (0, 2\pi]$ .

lattice of size  $L$ . In this manner, each component of the position of every individual can take any real number constrained to the area of the lattice, i.e.,  $x \in (0, L]$  and  $y \in (0, L]$ . Henceforth, let us set  $L = 1$ , such that  $N$  also corresponds to the density of organisms. The model assumes nonoverlapping generations, and individuals replicate with probability proportional to their fitness values.

More precisely, an individual that dies may be replaced by the offspring of any individual within a region centered on its location and delimited by the radius of competition,  $R$ . The probability that the focal individual is replaced by the offspring of individual  $i$  is given by

$$p_i = \frac{\omega_i}{\sum_{j \in A(R)} \omega_j}, \quad (1)$$

where  $\omega_i$  denotes the fitness of individual  $i$ , and the sum is taken over all individuals within the radius  $R$  (see Fig. 1). Individuals give rise to mutant offspring at rate  $U_b$ . Each new mutation increases the organism's fitness by a factor  $(1 + s)$ , where the selective effect  $s$  is from an exponential probability distribution with mean  $1/\alpha$ . The local competition, as defined, enables us to estimate the neighborhood population size as  $N_b = \pi R^2 N$ .

In the next stage, individuals diffuse over a fixed distance  $v$ . Nevertheless, the orientation  $\theta$  of the displacement is completely random,  $\theta \in (0, 2\pi]$ , and thereby the position vector changes as  $\vec{r}_{t+1} = \vec{r}_t + \vec{v}$ , which means that the change of the position components becomes  $\Delta x = v \cos \theta$  and  $\Delta y = v \sin \theta$ . Periodic boundary conditions are assumed.

As the initial condition, we consider that all individuals are mutation-free and have fitness equal to one. Their positions are randomly chosen. During simulations, we keep track of the evolutionary history of every mutation such that at the end we can estimate the quantities of interest, namely, the fixation rate ( $K_{\text{fix}}$ ), which corresponds to the number of mutations fixed divided by the time the population has evolved, and the mean selective effect of mutations that have been fixed in

the population ( $S_{\text{med}}$ ). Further, we store the trajectories of the log-fitness in order to estimate the speed of adaptation. In order to warrant a reasonable statistical accuracy, the simulations proceeded until at least 50 fixation events had been recorded.

### III. RESULTS AND DISCUSSIONS

We first analyze how the fixation probability of beneficial mutations,  $P_{\text{fix}}$ , depends on the model parameters. For these simulations, the population initially contains  $N - 1$  mutation-free individuals with fitness one and a single individual carrying a beneficial mutation with fitness  $1 + s$ . At this point, additional mutations do not occur and the population evolves to one of the absorbing states: loss of the mutation by genetic drift or its fixation, which means that all individuals share the mutation. We determined the dependence of  $P_{\text{fix}}$  on  $s$ . The results can be compared to the well-established theoretical prediction for an unstructured population, which states that the fixation probability  $P_{\text{fix}}$  is obtained through the numerical solution of the recursive equation

$$P_{\text{fix}} = 1 - \exp[-(1 + s)P_{\text{fix}}], \quad (2)$$

which was derived by means of the branching process formulation [1].

The left panel of Fig. 2 displays the fixation probability  $P_{\text{fix}}$  versus the selective effect  $s$  for different sets of the parameter values. The solid line is the theoretical prediction from Eq. (2). The prediction satisfactorily fits the simulation data whenever  $s$  has low values, regardless of the values of the other parameters. It is noticeable, though, that there is a slight discrepancy between prediction and simulations that becomes more evident when  $s$  is large and the dispersal velocity  $v$  and competition radius  $R$  are small. This result differs from what has been found in discrete lattice models with a fixed neighborhood (such as the von Neumann or Moore neighborhood [20]), where one obtains a good agreement between the theory and the simulation data over the whole range of selective effects  $s$ . Therefore, the present results reveal that the local structure

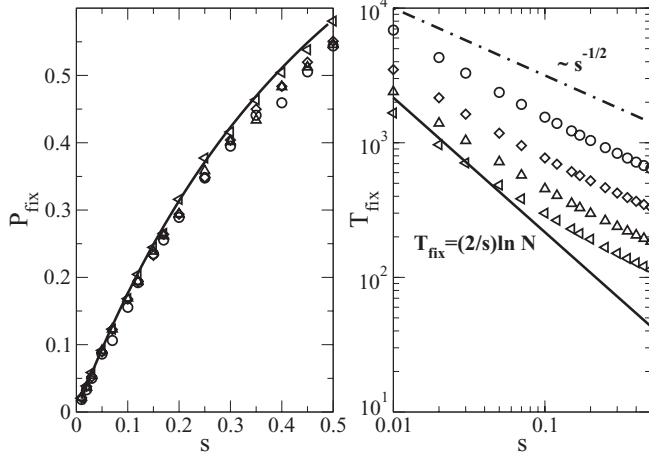


FIG. 2. Left panel: Fixation probability of a beneficial mutation as a function of its selective advantage  $s$ . The population size is  $N = 50\,000$ . The different symbols denote distinct sets of parameter values:  $v = 0.002$  and  $R = 0.005$  (circles),  $v = 0.005$  and  $R = 0.005$  (diamonds),  $v = 0.01$  and  $R = 0.005$  (triangles), and  $v = 0.005$  and  $R = 0.02$  (triangles point leftwards). The solid line corresponds to the branching process approximation for  $P_{\text{fix}}$  as given by Eq. (2). Right panel: Time to fixation of a beneficial mutation as a function of its selective advantage  $s$ . The set of parameters and symbols are the same as in the left panel.

of the population is relevant for the adaptive process in the regimes of low dispersal and limited competition radius.

Spatial population structure was introduced to the study of fixation by Maruyama [27]. Maruyama found that the fixation probability remains the same as in a panmictic population under the assumption of conservative migration. Conservative migration means that migration does not change local population sizes. Particularly, when the competition radius  $R$  and the dispersal parameter  $v$  are small, the conservative migration assumption is easily violated. Under these circumstances, individuals will frequently become isolated or interact with only a few other individuals over extended periods of time. On the other hand, when  $R$  is large, the number of individuals within the area delimited by  $R$  is also large, such that adjacent areas are continuously exchanging individuals, and stochasticity due to fluctuations in local population size is less intense.

It is well established that the fixation probability depends on the effective population size,  $N_e$ , which in turn is inversely proportional to the variance in offspring number. The dependence of  $P_{\text{fix}}$  on  $N_e$  is explicit in Kimura's formulation [41]. According to Kimura, the fixation probability is  $P_{\text{fix}} = \frac{1 - \exp(-2N_e s/N)}{1 - \exp(-2N_e s)}$  [41,42], which for small  $s$  becomes  $P_{\text{fix}} \approx 2s \frac{N_e}{N}$ . Because our results slightly deviate from the expectation of a homogeneous population, we may conclude that the effective population size  $N_e$  may be smaller than the census size  $N$ . Whenever the neighborhood size (number of individuals which compete locally) varies, it introduces an additional source of variation, which augments the variance in offspring number and consequently reduces the effective population size. This variance is expected to be larger for small  $R$  and  $v$ . Following Kimura, it is easy to see that for  $N_e$  sufficiently large, the discrepancy between the theoretical prediction and the

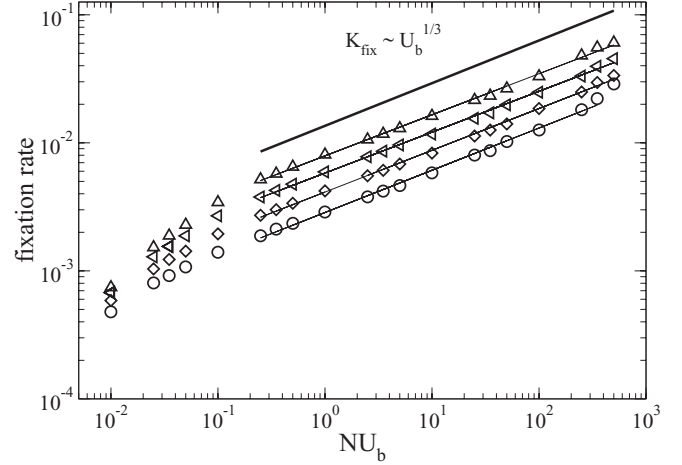


FIG. 3. Fixation rate  $K_{\text{fix}}$  versus (population size  $\times$  mutation rate)  $N \times U_b$ . The parameter values are population size  $N = 50\,000$ , mean selective effect  $1/\alpha = 0.05$ , dispersal parameter  $v = 0.005$ , and competition radius  $R = 0.0025$  (circles),  $v = 0.005$  and  $R = 0.005$  (diamonds),  $v = 0.005$  and  $R = 0.02$  (triangles), and  $v = 0.01$  and  $R = 0.005$  (triangles left).

simulation grows with  $s$  in the range of simulated  $s$  according to  $\Delta P_{\text{fix}} = \exp(-2s) - \exp(-2sN_e/N)$ .

Figure 2 (right panel) also shows the mean time to fixation versus  $s$  for the same set of parameters. As expected, the time to fixation reduces considerably as the dispersal parameter  $v$  grows. A similar role is played by the competition radius. For  $R = 0.02$  and small  $s$ , the times to fixation are very close to those expected for an unstructured population whose dependence on  $s$  is given by  $T_{\text{fix}} = (2/s) \ln N$  [40]. However, the decline of the fixation time with increasing  $s$  is proportional to  $s^{-1/2}$  and not to  $s^{-1}$  as in well-mixed populations. This result, which is independent of  $v$  and  $R$ , is consistent with previous results for spatially extended populations [22]. The local adaptation rule, as implemented, produces traveling waves at an average speed  $c \sim \sqrt{s}$ , which implies  $T_{\text{fix}} \sim s^{-1/2}$  [22,36,37] (see Fig. 4).

Henceforth, we concentrate on the adaptation dynamics if mutations are allowed to occur at a constant rate. Figure 3 shows the fixation rate  $K_{\text{fix}}$  versus the population-wide mutation rate  $N \times U_b$  for distinct sets of parameter values. Keeping the dispersal parameter  $v$  constant, we observe that  $K_{\text{fix}}$  increases with the competition radius  $R$ . Larger  $R$  also means a larger neighborhood population size  $N_b$ , which speeds up the spread of the mutation through the lattice, reducing the mean time to fixation. Smaller fixation time, in turn, reduces the likelihood of competition among established mutations (those that have overcome genetic drift), thus attenuating the strength of clonal interference [33]. From the same plot, we see that the fixation rate grows as one augments  $v$  (for essentially the same reasons). Most interestingly, at intermediate and large mutation rates, the increase of  $K_{\text{fix}}$  with  $U_b$  is well approximated by a power-law like  $K_{\text{fix}} \sim U_b^{1/3}$  regardless of the set of parameters. Thus, the power-law behavior seems to be related more to the dimensionality of the lattice than the details of the interactions among individuals [23].

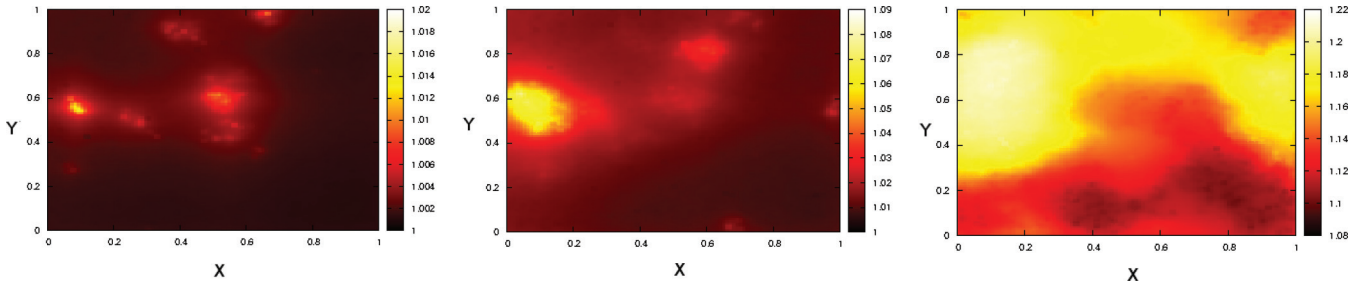


FIG. 4. (Color online) Snapshots of the distribution of individuals’ fitness across the lattice at three points in time:  $t = 100$  (left panel),  $t = 160$  (middle panel), and  $t = 300$  (right panel). The parameter values are population size  $N = 10\,000$ , mutation rate  $U_b = 1 \times 10^{-4}$ , mean selective effect  $1/\alpha = 0.05$ , competition radius  $R = 0.01$ , and dispersal parameter  $v = 0.005$ . Individuals’ fitness are color-coded (are represented in grayscale for the print version) according to the scale displayed in the bars along the right side of each panel.

Spatially structured population models are particularly interesting due to the wave-like spread of mutations. The situation is increasingly complex when mutation rates are high enough to enable the coexistence of established mutations, each one undergoing an expansion of its own. When the corresponding adaptive waves collide, a struggle for survival and dominance ensues, which entails the annihilation of “losing” mutations. This process turns clonal interference even more intense, bringing about a cost of adaptation for spatially structured populations when compared to well-mixed populations with the same characteristics [20,26,35]. Figure 4 shows snapshots of the spatial distribution of individuals’ fitness over the entire lattice at three different times. In generation  $t = 100$ , one can observe the rise of several distinct beneficial mutations (coded by lighter colors) with increased fitness in comparison to the genetic background. At a subsequent time ( $t = 160$ ), these mutants rise in frequency and disseminate as adaptive waves. Near the left border of the lattice, one observes the collision and interference of waves of different adaptive effects. At  $t = 300$  one still observes the interfering waves, but it is pretty clear that there is a dominant mutant type. Interference among adaptive waves effectively reduces the speed of their propagation, which does not depend on the selective effect of the mutant but rather on the fitness difference in the direction of the wave at the wave front. This means that an adaptive wave moves fastest on the wild-type genetic background.

Figure 5 shows the speed of adaptation, which is defined as  $V = \lim_{t \rightarrow \infty} \frac{\ln \bar{\omega}}{t}$  [34], against the beneficial mutation rate  $U_b$ .  $V$  is directly proportional to the fixation rate  $K_{\text{fix}}$  but also depends on the selective effects of the mutations that go to fixation. Nevertheless, the pattern is qualitatively similar to that shown in Fig. 3, and once again a power-law regime  $V \sim U_b^{1/3}$  emerges. The onset of the power-law regime is associated with that of the clonal interference regime. Clonal interference takes place when established mutations can coexist and compete for fixation. The onset of the regime can be found by determining the mutation rate at which the expected number of established mutations exceeds 1 during the time to fixation. Because the expected number of established mutations  $N_{\text{established}}$  is estimated as  $N_{\text{established}} = NU_b T_{\text{fix}} 2s$  for small  $s$ , and since  $T_{\text{fix}} \sim s^{-1/2}$ ,  $N_{\text{established}} \sim 2s^{1/2} NU_b$ . A characteristic value of fitness effects is  $s = 1/\alpha$ , and the onset of the clonal interference regime can be determined by

the condition  $2(\frac{1}{\alpha})^{1/2} NU_b \sim 1$ . For the same set of parameter values considered in Fig. 5, the onset of the clonal interference regime may occur around  $U_b \approx 4 \times 10^{-5}$ , which fits the simulation results very well.

The right panel of Fig. 5 shows that the log-fitness increases linearly with time, with a negligible period of initial transitory dynamics. Indeed, the slope of the line corresponds to the speed of adaptation. Figure 6 shows that the speed of adaptation (which has the same units as the mutation rate, i.e., generation<sup>-1</sup>) increases monotonically with the  $T_R = v/R$ . In the plot, we fixed the competition radius  $R$  and then varied the dispersal velocity  $v$ . An interesting feature is that a fixed  $R$  entails lower and upper bounds on the speed of adaptation, these limits being higher as larger competition radius  $R$  are considered. These results, together with those displayed in Fig. 2, suggest that  $v$  and  $R$  have different effects on the

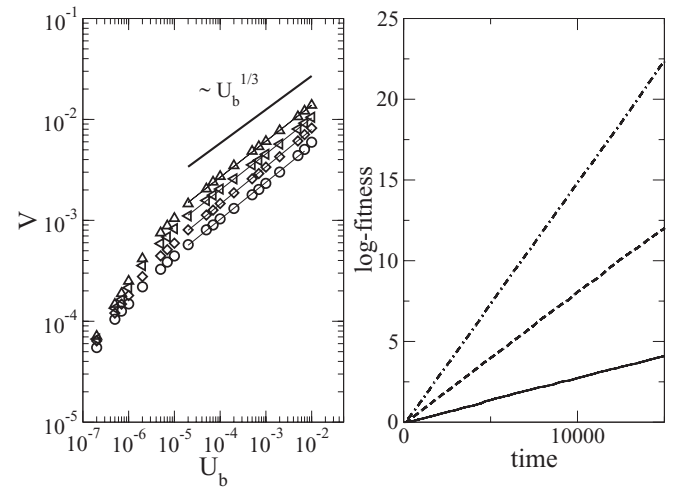


FIG. 5. Left panel: Speed of adaptation,  $V = \lim_{t \rightarrow \infty} \frac{\ln \bar{\omega}}{t}$ , versus mutation rate  $U_b$ . The parameter values and representation are the same as described in the legend of Fig. 3. Right panel: Log-fitness,  $\log(\bar{\omega})$ , over time for three distinct values of mutation rate  $U_b$ . The parameter values are population size  $N = 50\,000$ , mean selective effect  $1/\alpha = 0.05$ , dispersal parameter  $v = 0.005$ , and competition radius  $R = 0.005$ . The mutation rates are:  $U_b = 2 \times 10^{-6}$  (solid line),  $U_b = 2 \times 10^{-5}$  (dashed-line),  $U_b = 1 \times 10^{-4}$  (dot-dashed line). The lines are averages over 50 independent simulations.

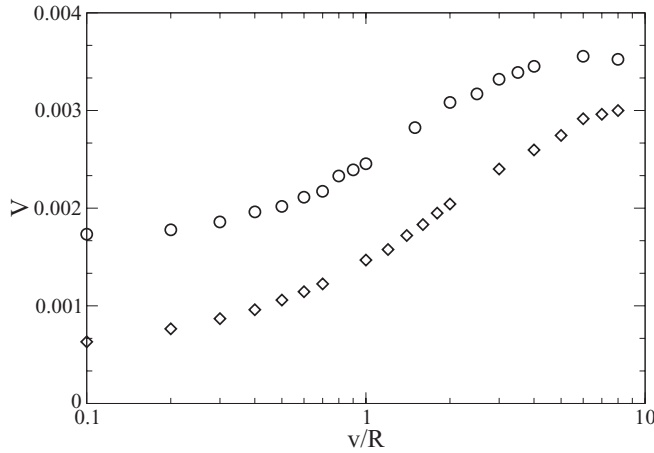


FIG. 6. Speed of adaptation,  $V = \lim_{t \rightarrow \infty} \frac{\ln \bar{w}}{t}$ , versus the ratio  $v/R$ , where  $v$  is the dispersal parameter and  $R$  is the competition radius. The parameter values are population size  $N = 50\,000$ , mean selective effect  $1/\alpha = 0.05$ , mutation rate  $U_b = 1 \times 10^{-4}$ , and competition radius  $R = 0.005$  (circles) and  $R = 0.01$  (diamonds). Data points are averages over 50 independent simulations.

adaptive evolution, with  $R$  developing a more prominent role in the homogenization of the system.

In Fig. 7 we plot the mean selective effect of those mutations that get fixed,  $s_{\text{med}}$ . For small values of  $v$  and  $R$ , the spread of beneficial mutations across the lattice is quite slow, and consequently clonal interference becomes intense. This leads to an increase in  $s_{\text{med}}$ , because only the best competitors survive in their struggle for fixation. For the same reasons,  $s_{\text{med}}$  increases with the mutation rate  $U_b$ . This pattern holds up to around  $U_b = 10^{-4}$ . Beyond this point, the converse happens, that is  $s_{\text{med}}$  decreases with  $U_b$  and increases with  $R$  and  $v$ , i.e., there exists a crossover behavior. Indeed, this point indicates the onset of the multiple mutation regime, where a lower fixation rate implies a greater chance of small effect mutations to hitchhike with those of large effect in their route to fixation.

Because the influx of beneficial mutations per generation is given by  $N \times U_b$ , another way to enhance adaptation (but also

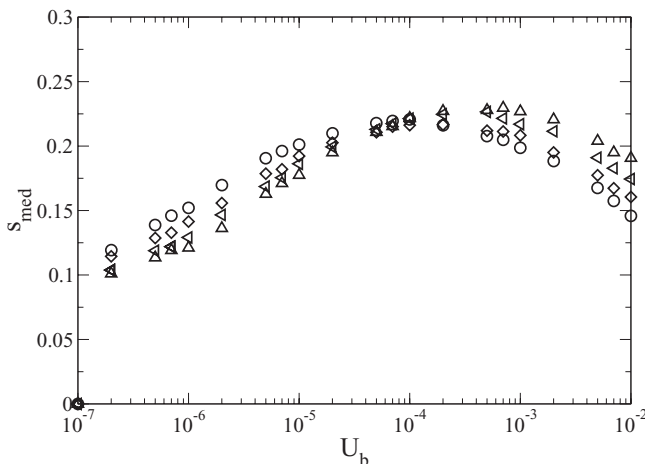


FIG. 7. Mean selective effect  $s_{\text{med}}$  of fixed mutations. The parameters are the same as described in the legend of Fig. 3.

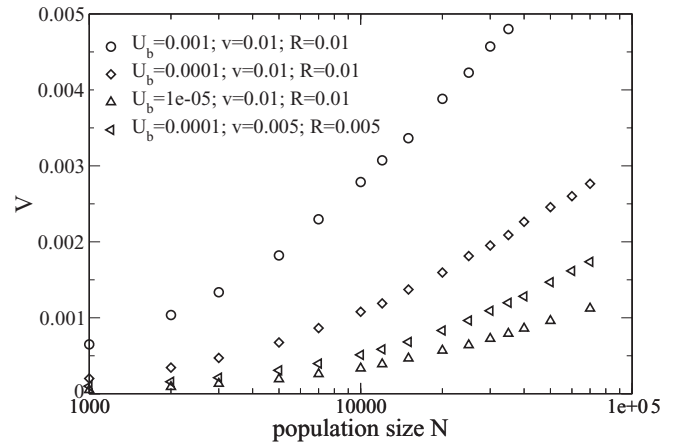


FIG. 8. Speed of adaptation,  $V = \lim_{t \rightarrow \infty} \frac{\ln \bar{w}}{t}$ , versus population size  $N$ . The parameter values are indicated in the figure. Note that, in contrast to Fig. 7, the  $V$  axis is linear, not logarithmic.

clonal interference), for a fixed mutation rate  $U_b$ , is to enlarge the population size  $N$ . For intermediate to large population sizes,  $V$  increases logarithmically with  $N$  (Fig. 8), which contrasts with the power-law-like dependence on  $U_b$  (Fig. 7). Previous studies of spatially extended populations in discrete lattices [19,22] showed that the speed of adaptation saturates when the population size attains a characteristic scale  $L_c$ , a fact not observed in the continuous model presented in the paper. In the former, the neighborhood size is constant regardless of the linear size  $L$ , and as the system size is augmented, longer times to fixation ensue, and hence enhancing the expected number of established mutations that can coexist. Additionally, larger system sizes mean larger regions of contact between spreading waves, also enhancing the clonal interference strength. On the other hand, in the continuous model an increased  $N$  corresponds to a larger density of individuals but not that the systems extends over larger areas. As such, the effective neighborhood size augments and so each individual has a larger number of local interactions, which has a homogenizing effect. In this way, it is expected that the continuous population model behaves similarly to well-mixed populations, where a logarithmic growth of the speed of adaptation  $V$  with the population size  $N$  (also denoting density) is observed [10,34].

#### IV. CONCLUSIONS

In summary, we have proposed a continuous lattice model to investigate the adaptive evolution of a spatially structured population. In contrast to standard discrete lattice models with a well-defined fixed neighborhood, here the neighborhood size (number of individuals that compete locally) varies over time.

Our simulation results show that these new assumptions do not alter significantly the fixation probabilities of beneficial mutations with small fitness effects  $s$ . Furthermore, in the range of parameter values we explored, the mean time required for the fixation of a beneficial mutation is proportional to  $s^{-1/2}$ , implying that the speed of the genetic wave front is  $c \sim \sqrt{s}$ . Our model is, thus, consistent with the weak-noise [36] rather than the strong-noise regime  $c \sim s$  [38].

We obtained that both the fixation rate and the speed of adaptation display a power-law dependence on mutation rate  $U_b$  (i.e., proportional to  $U_b^{1/3}$ ), at least for intermediate and large  $U_b$ , and irrespective of the other parameter values. Similar results have been previously found in a discrete lattice model [22]. When studying the mean selective effect of fixed mutations ( $s_{\text{med}}$ ) as a function of  $U_b$ , we observe a crossover point delimiting the clonal interference and multiple mutation regimes.

Finally, an interesting feature of the model is that the speed of adaptation grows logarithmically with the population size, consistent with previous derivations for well-mixed populations [10,34]. This result contrasts with the one previously reported for spatially extended populations in discrete lattices, in which the speed of adaptation saturates and reaches an upper bound with increasing population sizes [19,22]. Therefore, we

may conclude that the present spatial model on a continuous lattice exhibits a dual character and shows aspects of both spatially structured populations and well-mixed populations, which can be tuned by varying the competition radius and dispersion velocity.

#### ACKNOWLEDGMENTS

This work was partially supported by the Brazilian research agencies CNPq, CAPES, and FINEP. P.R.A.C. acknowledges financial support from the program PRONEX/MCT-CNPq-FACEPE and Fundação de Amparo à Ciência e Tecnologia do Estado de Pernambuco (FACEPE). M.L.L. acknowledges the partial support provided by the Alagoas state research agency FAPEAL.

- 
- [1] J. B. S. Haldane, *Proc. Camb. Phil. Soc.* **26**, 220 (1927).  
 [2] R. A. Fisher, *The Genetical Theory of Natural Selection* (Oxford University Press, Oxford, 1930).  
 [3] R. E. Lenski and M. Travisano, *Proc. Natl. Acad. Sci. USA* **91**, 6808 (1994).  
 [4] J. E. Barrick, D. S. Yu, S. H. Yoon, H. Jeong, T. K. Oh, D. Schneider, R. E. Lenski, and J. F. Kim, *Nature (London)* **461**, 1243 (2009).  
 [5] L. Perfeito, L. Fernandes, C. Mota, and I. Gordo, *Science* **317**, 813 (2007).  
 [6] S. F. Elena and R. E. Lenski, *Nat. Rev. Genet.* **4**, 457 (2003).  
 [7] J. Felsenstein, *Genetics* **78**, 737 (1974).  
 [8] M. M. Desai, D. S. Fisher, and A. W. Murray, *Curr. Biol.* **17**, 385 (2007).  
 [9] H. J. Muller, *Am. Nat.* **66**, 118 (1932).  
 [10] H. Sayama, L. Kaufman, and Y. Bar-Yam, *Phys. Rev. E* **62**, 7065 (2000).  
 [11] P. Klimek, S. Thurner, and R. Hanel, *Phys. Rev. E* **82**, 011901 (2010).  
 [12] M. A. M. de Aguiar and Y. Bar-Yam, *Phys. Rev. E* **84**, 031901 (2011).  
 [13] J. Mathiesen, N. Mitarai, K. Sneppen, and A. Trusina, *Phys. Rev. Lett.* **107**, 188101 (2011).  
 [14] C. Borile, M. A. Muñoz, S. Azaele, J. R. Banavar, and A. Maritan, *Phys. Rev. Lett.* **109**, 038102 (2012).  
 [15] D. B. Saakian, Z. Kirakosyan, and C.-K. Hu, *Phys. Rev. E* **86**, 031920 (2012).  
 [16] E. H. Colombo and C. Anteneodo, *Phys. Rev. E* **86**, 036215 (2012).  
 [17] R. A. Neher, B. I. Shraiman, and D. S. Fisher, *Genetics* **184**, 467 (2010).  
 [18] N. Colegrave, *Nature (London)* **420**, 664 (2002).  
 [19] J. Otwinowski and S. Boettcher, *Phys. Rev. E* **84**, 011925 (2011).  
 [20] I. Gordo and P. R. A. Campos, *Genetica* **127**, 217 (2006).  
 [21] M. G. J. L. Habets, T. Czárán, R. F. Hoekstra, and J. A. G. M. de Visser, *Proc. R. Soc. B* **274**, 2139 (2007).  
 [22] E. A. Martens, R. Kostadinov, C. C. Maley, and O. Hallatschek, *New J. Phys.* **13**, 115014 (2011).  
 [23] E. A. Martens and O. Hallatschek, *Genetics* **189**, 1045 (2011).  
 [24] P. Watnick and R. Kolter, *J. Bacteriol.* **182**, 2675 (2000).  
 [25] T. Tolker-Nielsen and S. Molin, *Microb. Ecol.* **40**, 75 (2000).  
 [26] L. Perfeito, M. I. Pereira, P. R. A. Campos, and I. Gordo, *Biol. Lett.* **4**, 57 (2007).  
 [27] T. Maruyama, *Genet. Res.* **15**, 221 (1970).  
 [28] Z. Patwa and L. M. Wahl, *J. R. Soc. Interface* **5**, 1279 (2008).  
 [29] P. R. A. Campos, P. S. C. A. Neto, V. M. de Oliveira, and I. Gordo, *Evolution* **62**, 1390 (2008).  
 [30] S. Manel, M. K. Schwartz, G. Luikart, and P. Taberiet, *TRENDS Ecol. Evol.* **18**, 189 (2003).  
 [31] R. Holderegger and H. H. Wagner, *Landscape Ecol.* **21**, 793 (2006).  
 [32] J. N. Amos, A. F. Bennett, R. C. Naily, G. Newell, A. Pavlova, J. Q. Radford, J. R. Thomson, M. White, and P. Sunnucks, *Plos One* **7**, e30888 (2012).  
 [33] P. D. Sniegowski and P. J. Gerrish, *Phil. Trans. R. Soc. B* **365**, 1255 (2010).  
 [34] Su-Chan Park, D. Simon, and J. Krug, *J. Stat. Phys.* **138**, 381 (2010).  
 [35] A. Rosas, I. Gordo, and P. R. A. Campos, *Phys. Rev. E* **72**, 012901 (2005).  
 [36] R. A. Fisher, *Ann. Eugen.* **7**, 355 (1937).  
 [37] A. N. Kolmogorov, I. Petrovsky, and N. Piscounov, *Moscow Univ. Bull. Math.* **1**, 1 (1937).  
 [38] O. Hallatschek and K. S. Korolev, *Phys. Rev. Lett.* **103**, 108103 (2009).  
 [39] K. S. Korolev, M. Avlund, O. Hallatschek, and D. R. Nelson, *Rev. Mod. Phys.* **82**, 1691 (2010).  
 [40] M. Kimura and T. Ohta, *Genetics* **61**, 763 (1969).  
 [41] M. Kimura, *J. Appl. Prob.* **1**, 177 (1964).  
 [42] S. P. Otto and M. C. Whitlock, *Genetics* **146**, 723 (1997).